CRYSTAL GROWTH & DESIGN
2005
VOL. 5, NO. 5
1801−1806

Shape-Controlled Synthesis of CdS Nanocrystals in Mixed Solvents

Haibin Chu, Xuemei Li, Guangda Chen, Weiwei Zhou, Yan Zhang, Zhong Jin, Junjian Xu, and Yan Li*

Key Laboratory for the Physics and Chemistry of Nanodevices, College of Chemistry and Molecular Engineering, Peking University, Beijing 100871, China

Received February 26, 2005; Revised Manuscript Received May 8, 2005

ABSTRACT: The formation of CdS nanotetrahedrons, pencil-shaped nanorods, tetrapods, prickly spheres, and high aspect-ratio hexagonal nanoprisms has been, respectively, achieved by adjusting the ratio of two solvents ethylenediamine and ethylene glycol under the solvothermal condition. None of the surfactants or other templates was needed in the process. The reaction time and temperature can be used as the additional means to control the size and morphology. By closely inspecting the growing process of the tetrapod structure and the crystallographic analysis of the products, we proposed that the lattice space match and the location match of ions at the interface of the zinc blende core and the wurtzite arms are two important structural factors to guide this furcate growth. Also, the anisotropic adsorption ability of ethylenediamine at the different surfaces of wurtzite CdS crystals results in the 1D growth of the arms. The possible growing mechanisms of CdS with other shapes were also discussed.

Introduction

Recent studies have shown that many fundamentally physical properties of semiconductor materials strongly depend on the size, shape, and structure of the semiconductor nanocrystals.[1−5] Thus, to establish well-controlled synthetic methods and to understand the mechanisms by which the size and shape of the nanocrystals can be easily varied are key issues in nanoscience. As a kind of important II-VI group semiconductor material, CdE (E = S, Se, Te) nanocrystals have important potential applications in solar cells,[6] light-emitting diodes (LEDs),[7,8] nonlinear optical materials,[9] optoelectronic and electronic devices,[10] biological labeling,[11−13] etc. The preparation of supra-structures based on nanorods would offer both opportunities to exploit the distinctive optical and electronic properties of the discrete 1D nanostructures[3−5,10] and possibilities to probe potentially new phenomena arising from their 2D or 3D organization.[14,15]

For the past few years, various methods have been developed for the morphology control of semiconductor nanocrystals. For example, a well-controlled synthetic scheme to prepare CdSe nanocrystals with different morphology by thermal decomposition of organometallic precursors in a hot mixture of binary surfactants had been developed by Alivisatos et al.[4,16] By the combined control of the monomer concentration, surfactant ratio, injection volume, reaction temperature, and reaction time, the shape could be varied from hexagon, rod, arrow, teardrop, to multi-armed rod. This organometallic approach had been further developed by Peng et al., in which the shape evolution of the CdSe nanocrystals was effectively accounted for by employing a safe alternative precursor and proposing a three-staged mechanism that was different from the Ostwald ripening mechanism.[17−19] Cheon et al. found that the crystalline phase of nucleating seeds and the kinetic growth regimes were crucial for the determination of the 1D geometry of nanocrystals when they used a mono-surfactant system to achieve the goal.[20,21] By using various solvents in the solvothermal process, Qian and his group had drawn the conclusion that ethylenediamine (en) played a key role in the formation of CdS nanorods.[22,23] Li et al. pointed out that the morphology of the resultant CdS nanoparticles could be determined by shifting the reactions between thermodynamically controlled and kinetically controlled.[24]

Most of the synthetic schemes described above required the use of rather complicated procedures or the presynthesis of cluster precursors. The subsequent research focused mainly on the temperature, precursor concentration, and reaction time to control the shape of the CdE nanocrystals.[20,24] Our idea is to use mixed solvents with distinct properties to achieve the morphology modulation. We chose ethylenediamine (en), in which normally CdS nanorods with wurtzite structure were obtained,[22,23] and ethylene glycol (EG), in which CdS nanoparticles with zinc blende structure were obtained.[25] By just simply adjusting the volume ratio of the above two solvents, the CdS morphology can be easily varied.

Experimental Section

All of the reactants and solvents are of analytical-grade and are used without further purification. In a typical process, cadmium acetate ($Cd(CH_3COO)_2 \cdot 2H_2O$, 0.38 g, 1.4 mmol) and thioacetamide (CH_3CSNH_2, TAA, 0.15 g, 2.0 mmol) were added into a Teflon-lined stainless steel autoclave, which had been filled with aforehand mixed and cooled solvents of en and EG to 70% of its capacity. No surfactant or other additives were used here. The autoclaves were taken out of the furnace after the reaction had been carried out at 180 °C for 5 h. They were then cooled to room temperature. The yellow precipitates were washed with absolute alcohol and distilled water several times to remove the excessive reactants and byproducts, followed by drying in a vacuum at 70 °C for 1 h. The yellow powders were collected for characterization.

X-ray diffraction (XRD) patterns were obtained on a Rigaku Dmax-2000 X-ray diffractometer with graphite monochroma-

* Corresponding author. Phone/fax: +86-10-62756773. E-mail: yanli@pku.edu.cn.

10.1021/cg050068w CCC: $30.25
Published on Web 08/19/2005

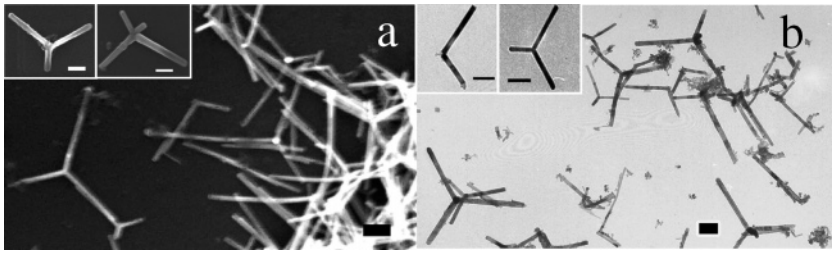

Figure 1. SEM and TEM images of CdS products obtained at 180 °C for 5 h with 50% en in the mixed solvents. (a) SEM image with insets showing individual tripod and tetrapod; (b) TEM image with insets showing a bipod and a tripod. Scale bar = 100 nm.

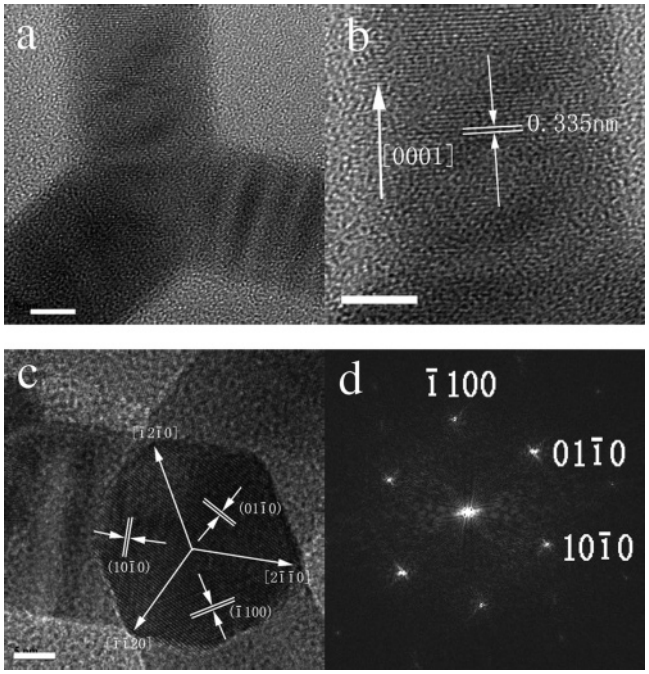

Figure 2. HRTEM images of the multi-armed structures. (a) HRTEM image of a tripod; (b) the magnified image of the upper arm in (a); (c) HRTEM image of a tetrapod; (d) FFT pattern recorded from the dark area in the image. Scale bar = 5 nm.

tized Cu Kα radiation ($\lambda = 1.5406$ Å). The accelerating voltage was set at 40 kV with 100 mA flux at a scanning rate of 8°/min in the 2θ range of 10−70°. Transmission electron microscopy (TEM) and selected area electron diffraction (SAED) were taken with a JEOL-200CX transmission electron microscope using an accelerating voltage of 160 kV. High-resolution transmission electron microscopy (HRTEM) was taken on an H-9000 NAR transmission electron microscope. Samples were prepared by placing a drop of dilute alcohol suspension of the products onto a carbon-coated copper grid and allowing the alcohol to evaporate in air. Scanning electron microscopy (SEM) was taken on an SL30 S-FEG scanning electron microscope, using an accelerating voltage of 160 kV.

Results and Discussion

Figure 1 shows SEM and TEM images of multi-armed nanostructures obtained under the typical condition with 1:1 (v:v) en and EG as the solvent. The product was mainly made of bipods, tripods, and tetrapods. Some monopode rods (less than 20%) were also found in the sample (Figure 1a,b), which is similar to those shown previously in the literature.[20,26,27] HRTEM images in Figure 2 recorded on the tripods and tetrapods provided further insight into their structures. The distances of the lattice space perpendicular to the growing directions indicate that the structures extend along the [0001] direction of wurtzite CdS, which is consistent with those reported in the literature.[20,27−29] We were very lucky to find a tetrapod with a very short arm so that we could look into the microstructure of the (0001) plane perpendicular to the growing direction. Figure 2c shows clearly the surface plane lattice of the arm pointing to the observers. The crystal plane spaces of all of these three sets of planes were calculated to be 0.35 nm, which is quite similar to the d value of (100) of the wurtzite CdS. Thus, these three sets of planes could be ascribed to the $(10\bar{1}0)$, $(01\bar{1}0)$, $(\bar{1}100)$ planes, respectively, with the growing directions of $[2\bar{1}\bar{1}0]$, $[\bar{1}\bar{1}20]$, $[\bar{1}2\bar{1}0]$, which is reconfirmed by two-dimensional fast Fourier transform (FFT) of the lattice resolved image of this special area as illustrated in Figure 2d. Further analysis of this special surface structure may throw light on the growing process of the multi-armed structures.

To investigate the morphology evolution during the growth of the multi-armed rods, we performed the synthesis at 150 °C with 1:1 (v:v) of en and EG as the solvent under different reaction time. The TEM images are shown in Figure 3. At the very early stage of 0.5 h, the shape of the products shown in Figure 3b was quite similar to the samples obtained in the pure EG for 5 h shown in Figure 3a, but the average particle size of the former products is only about 8 nm, and the latter is 13 nm. When the reaction time increased from 0.5 to 1.0 h, the nanoparticles changed into small multi-armed structures with arms of about 20 nm in length and about 10 nm in diameter (Figure 3c). The length increased to about 40 nm, and the diameter increased to about 15 nm at 1.5 h (Figure 3d). When the reaction time was further prolonged, the length of the arms kept on increasing quickly while the diameter increased at a much lower rate. It should be clarified here that the shape of the products in pure EG would not change any more as the reaction time was longer than 5 h.

We systematically studied the effect of the volume ratio of en and EG on the morphology of the resultant CdS. TEM and SEM images of the samples obtained at 180 °C using mixed en and EG with a volume ratio other than 1:1 as solvents are shown in Figure 4. The typical shapes and corresponding dimensional parameters of the different products are listed in Table 1. More results are shown in the Supporting Information. As shown in Figure 4a, small particles were obtained in solvent containing 5% v/v of en. Nanoparticles were also obtained in pure glycol.[25] However, the particles prepared in pure EG are almost spherical, but most of the particles are tetrahedral when 5% en was introduced.

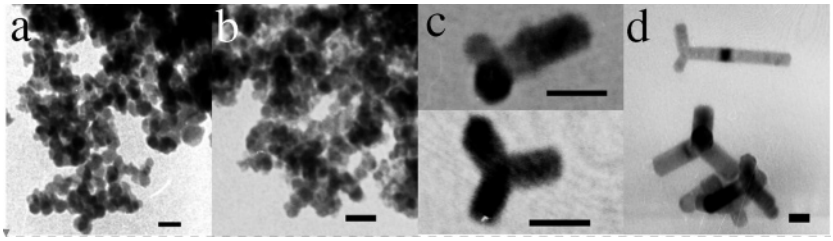

Figure 3. TEM images of CdS products obtained at 150 °C: (a) in the solvent of pure EG for 5 h; (b−d) in the solvent containing 50% en for 0.5, 1.0, and 1.5 h, respectively. Scale bar = 20 nm.

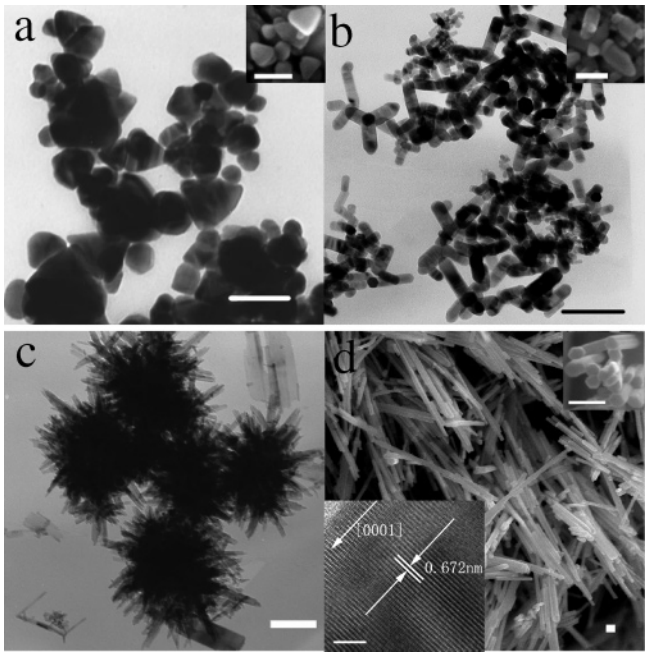

Figure 4. TEM and SEM images of CdS products obtained at 180 °C for 5 h in mixed solvents with different volume ratios: (a) 5% of en, TEM image with SEM image as inset; (b) 15%, TEM image with SEM image as inset; (c) 65%, TEM image; (d) 100%, SEM image with the upper right inset showing a magnified picture of the hexagonal ends of the long rods, and the lower left inset showing the HRTEM image of a nanorod. The scale bars in the TEM and SEM images all represent 100 nm. The scale bar in the HRTEM image is 5 nm.

Table 1. Summarized Morphologies and Sizes of CdS Obtained under Different Solvent Composition

sample	ratio of en	morphology	rod size ($L \times D$, nm)	L/D
1	5%	tetrahedrons and spheres	64[a]	1
2	15%	pencil-shaped rods	49 × 20	2.45
3	50%	multiarmed nanostructures	206 × 22.5[b]	9.16
4	65%	prickly spheres	*c*	*c*
5	100%	hexagonal nanoprisms	748 × 35	21.4

[a] The average diameter of the spheres and the length of the tetrahedral edges. [b] Data of each arm. [c] The sizes of the rods making prickly spheres are difficult to measure.

Estimated from over 50 particles, the average size (diameter of the spheres and the length of the tetrahedral edges) is 64 nm. When the en ratio was 15%, pencil-shaped rods with the average dimensional sizes of 49 nm × 20 nm were obtained (Figure 4b). When the en ratio increased to 50%, multi-armed nanostructures were obtained as shown in Figure 1. When the ratio of en was 65%, prickly spheres made of rods were obtained (Figure 4c). Long rods were found in majority in pure

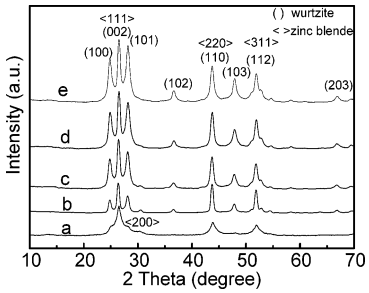

Figure 5. XRD patterns of CdS products obtained under 180 °C for 5 h in mixed solvents with the en volume ratios of 0% (a), 5% (b), 15% (c), 50% (d), and 65% (e).

en (Figure 4d), which is quite consistent with that Qian et al. reported.[22,23] Close inspection of the ends of the rod in the upper right inset in Figure 4d shows that they are hexagonal prisms. The hexagonal cross-section is considered to be the (0001) crystal face of hexagonal CdS, and the length direction of the rods is along [0001] as shown in the lower left inset of Figure 4d. It was found from Table 1 that, besides the variation of appearance, the aspect ratio of the products increases with the increase of the en content.

The XRD patterns (Figure 5) showed that the crystalline phase of the products changed as the ratio of the two solvents differed. The product obtained in pure EG was mainly made of zinc blende phase CdS (JCPDS 80-0019). Along with the increase of en content in the solvent, the intensity of the characteristic peak of zinc blende phase at $2\theta = 30.75°$ ($d = 2.90$ Å, ⟨200⟩) decreased obviously, and almost disappeared at last. Meanwhile, the relative ratio of peaks at $2\theta = 28.33°$, which is the characteristic (101) peak of wurtzite CdS, to the peaks at $2\theta = 26.51°$, which corresponds to the diffraction peaks in both wurtzite and zinc blende phases, increased. These changes indicate that when the ratio of en in the mixed solvent increases, the wurtzite phase of CdS increases while the zinc blende phase decreases in the products, and at last only wurtzite phase CdS (JCPDS 41-1049) is obtained. So, we proved again that en is in favor of the formation of wurtzite CdS and EG is beneficial for the formation of zinc blende CdS. We know that there is a very strong coordination interaction between en and Cd^{2+}. Cd^{2+} in the solvent of en intended to form a gauche conformation of $Cd(en)_3^{2+}$ with a quite large cumulative formation constant $\log K_3 = 12.09$ at 25 °C, while the $\log K_3$ of cadmium acetate is only 2.4 (from *Lang's Handbook of Chemistry*, 15th ed.). Therefore, the concentration of isolated Cd^{2+} in the en solution was so small that the formation of CdS would be at a rather low rate. The thermodynamic stable wurtzite phase was thus obtained in en. However,

the decrease of Cd^{2+} concentration would not take place in EG, so the product with zinc blende phase, which is in kinetic priority, was obtained.

As we already know that zinc blende CdS nanoparticles are obtained in pure EG[25] and wurtzite CdS nanowires are obtained in pure en,[22,23] therefore, from the morphological change of the products with the en and EG ratio and the reaction time in 1:1 mixed solution of en and EG, we can propose the growth mechanism of multi-armed nanostructures. First, tiny CdS nanoparticles with zinc blende structure are formed in the mixed solution because zinc blende phase is in kinetic priority; soon after that, the preformed zinc blende CdS nanoparticles act as the seeds and wurtzite arms grow from them. It is known that the locations of the Cd^{2+} and S^{2-} ions on the (111) plane of zinc blende CdS are just identical to the locations of the ions on the (0001) plane of wurtzite CdS. Furthermore, some crystal planes in the zinc blende CdS are correlative with some crystal planes in the wurtzite CdS due to their relation in the d values, such as

$$d_{ZB(111)} = d_{W(002)} = 3.3549 \text{ Å}$$

$$2d_{ZB(311)} = d_{W(100)} = 3.5861 \text{ Å}$$

So the {0001} planes of the wurtzite arms can fit well with the already formed {111} planes of the zinc blende core. Also, the $(10\bar{1}0)$, $(01\bar{1}0)$, $(\bar{1}100)$ planes in the wurtzite structured arms can fit well with the already formed {311} planes in the zinc blende structured core. Both location match and lattice space match lead to the multi-armed growth, which is consistent with the model in the literature.[30] The function of the en should be emphasized here. In Qian's work,[23] they had proved by IR that the en molecules coordinate with Cd^{2+} using trans conformation on the surface of CdS. This coordination could slow the growth speed of the crystal planes. Different planes of the nanocrystals have different adsorption ability.[18,26] The planes that have fewer attached en molecules grow more rapidly than those with more. As a result, they tend to assemble one by one to form a specific shape. In this situation, en tends to attach to the $\{10\bar{1}0\}$ planes and suppress the growth rate of these planes, and the (0001) plane covered with the least en grows fastest. Thus, it is the different adsorption ability of en on different planes of CdS nanocrystals that makes the 1D growth of wurtzite arms possible. In a typical case, the four wurtzite arms grow out of the four (111) equivalent faces of the tetrahedral zinc blende core under the inducement of en. Completely identical arms should be formed in the ideal case. However, due to the heterogeneity of the micro-environment formed somehow during the reaction, the inequilateral growth may take place; therefore, mixed structures of two-, three-, four-armed structures were found in the products, and the arm lengths in the tetrapods might be different. The Ostwald ripening process, in which the longer arms grew even longer in the sacrifice of the shorter arms, may also contribute to the inequality of the final products.

To make sure of the growth mechanism, we isolated the zinc blende CdS products synthesized in pure EG. After washing with absolute alcohol and distilled water several times, we added them into a Teflon-lined autoclave to conduct the typical solvothermal process as described in the Experimental Section. Multi-armed and mono-armed rods were obtained when the solvent was pure en (see Supporting Information). A similar result was obtained when we used the sample synthesized in 1:1 v/v en/EG for 30 min as the seeds to carry out the synthesis in pure en (see Supporting Information). These results well confirm the mechanism we proposed.

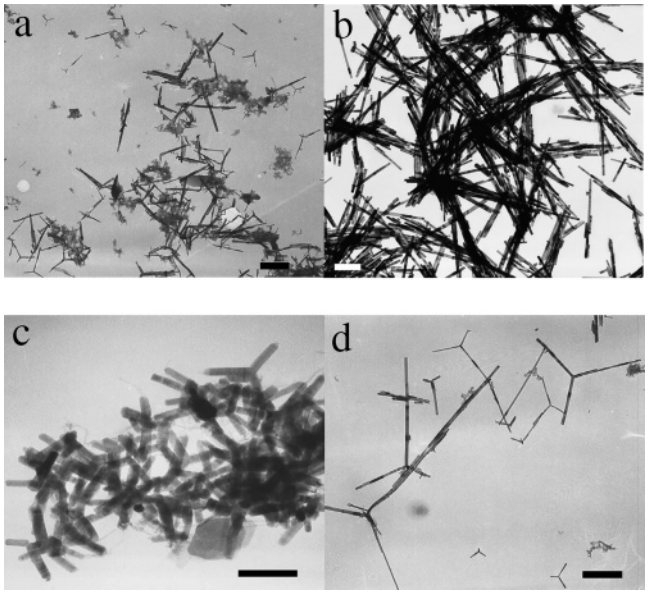

Figure 6. TEM images of CdS products obtained under different conditions with the en ratio of 65%: (a) 160 °C, 5 h, multi-armed structures, 100−600 nm in arm length, 20 nm in diameter; (b) 210 °C, 5 h, long rods; (c) 160 °C, 1 h, multi-armed structures, 80−100 nm in arm length, 20 nm in diameter; (d) 160 °C, 11 h, multi-armed structures, 100−1500 nm in arm length, 20−30 nm in diameter. Scale bar = 100 nm.

The energy difference of the two phases of CdS is very small,[26] which makes it difficult to controllably isolate the growth of one phase at a time. However, it also makes it easy for producing complex structures. In our case, mixed solvents of en and EG with different volume ratios were used as reaction media, each producing a distinguished morphology of obtained CdS. What is more, en intends to bring on the formation of one-dimensional CdS nanorods. Thus, it is understandable that the aspect ratio of the length to the diameter of the rods increased with the increase of en content. In typical compositions of these two solvents, the possible crystal growing processes are discussed as follows. When the ratio of en is 5%, the concentration of en is too low to induce the one-dimensional growth of CdS. Yet the amount of en is enough to coordinate with most of Cd^{2+}, which would highly reduce the Cd^{2+} concentration in the system. So the crystals are inclined to grow along four (111) equivalent faces of the zinc blende structure to shape tetrahedrons. When the ratio of en is higher, that is, 7−35%, one crystal face of the tetrahedral core with relatively low surface energy may lead to the mono-directional growth of wurtzite CdS rods and give off pencil-shaped products, which is quite different from the high aspect-ratio hexagonal prisms formed in pure en. Multi-armed nanostructures are obtained when the ratio of en is between 35% and 70%, and this shape is the result of relatively high concentra-

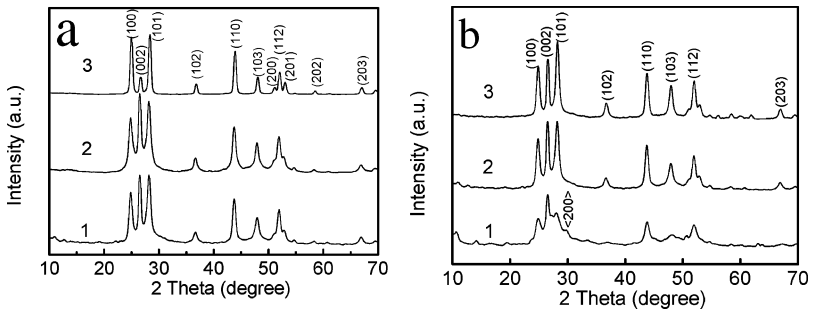

Figure 7. XRD patterns of CdS products obtained with the en content of 65%: (a) for 5 h under the temperatures of 160 °C (1), 180 °C (2), and 210 °C (3); (b) under 160 °C at the reaction time of 1 h (1), 5 h (2), and 11 h (3).

tion of both solvents as discussed formerly. When the ratio of en is about 65%, the nucleation stage is similar to the case in 1:1 mixed solvent. However, in the following stage of morphology-reforming, the concentration of Cd^{2+} would be lower than that in 1:1 mixed solvent as there are higher concentrations of en. Thus, this crystal growing stage would favor the diffusion-limited aggregation (DLA) mechanism.[31,32] Combined with the one-dimensional inducement by en, the intense diffusion and exchange among the growing rods result in the formation of prickly spheres. When the ratio of en is even higher, the concentration of Cd^{2+} becomes even lower. Also, it is hard to form zinc blende structures in relatively low content of EG. Henceforth, high aspect-ratio hexagonal nanoprisms are obtained just like in pure en.

Although the samples prepared through our simple method with mixed solvents are not as uniform as that obtained by the precursor thermal decomposition method, the shape of CdS nanorod architectures can be adjusted in a wide range. Furthermore, the reaction temperature and reaction time can be employed as additional parameters to help to control the shape as well as the size of these structures. We chose the reaction system containing 65% en to test this. When we kept the reaction time at 5 h, we obtained multi-armed structures at 160 °C as shown in Figure 6a, prickly spheres at 180 °C as shown above in Figure 4c, and nanorods at 210 °C as shown in Figure 6b. When we kept the reaction temperature at 160 °C, we found the arm length of the multi-armed structures increased gradually from 80 to 100 nm at 1 h (Figure 6c), 100−600 nm at 5 h (Figure 6a), to 100−1000 nm at 11 h (Figure 6d). The length distribution of the sample formed within 1 h was nearly monodisperse, but it became broader as the reaction time was prolonged. This was presumably because the arm, which was even slightly larger than the others, could consume the smaller ones in the Ostwald ripening process. We found again that there was little change in the arm diameter with the increase of reaction time. It seems that lower reaction temperature is beneficial for the formation of multi-armed structures. This is probably because that low temperature is favorable for the formation of the initial CdS seeds with zinc blende structure, which is thermodynamically unstable but kinetically preferential. This can be proved from the XRD patterns of the CdS products obtained at different time and temperature in Figure 7. The characteristic peaks of zinc blende phase were found in the samples of 160 °C, especially in the sample obtained at the very short reaction time of 1 h. Yet no such peaks were found in the samples obtained at higher temperatures.

Conclusion

In summary, a simple and novel route for controlling the morphology and size of CdS nanocrystals has been developed. The mixed solvents of ethylenediamine, which is propitious to the formation of wurtzite CdS with high aspect ratio, and ethylene glycol, which is favorable for the formation of zinc blende CdS with low aspect ratio, were used to obtain CdS of varied morphologies under solvothermal conditions. The solvent ratio as well as reaction time and temperature provide us with methods by which we can prepare nanostructured CdS of different architectures. It is highly possible that this scheme can be extended as a general synthetic method for other nanocrystals if their structures show the existence of different phases in different solvents. This also may be a short road to exploit new morphology with polytypic structures for many materials.

Acknowledgment. We would like to thank Dr. Xiaodong Zou of Stockholm University for helpful discussion about the HRTEM result. This work was supported by NSFC, MOE, and MOST (Project 2001-CB610501) of China.

Supporting Information Available: Morphology change at different en and EG ratios, the tetrapods formed in pure en with the preformed zinc blende CdS as the seeds, and the photoluminescence study of the products. This material is available free of charge via the Internet at http://pubs.acs.org.

References

(1) Chen, C. C.; Herhold, A. B.; Johnson, C. S.; Alivisatos, A. P. *Science* **1997**, *276*, 398.
(2) (a) Yu, W. W.; Peng, X. G. *Angew. Chem., Int. Ed.* **2002**, *41*, 2368. (b) Poznyak, S. K.; Talapin, D. V.; Shevchenko, E. V.; Weller, H. *Nano Lett.* **2004**, *4*, 693.
(3) Burda, C.; Chen, X.; Narayanan, R.; El-Sayed, M. A. *Chem. Rev.* **2005**, *105*, 1025.
(4) Peng, X. G.; Manna, L.; Yang, W. D.; Wickham J.; Scher, E.; Kadavanich, A.; Alivisatos, A. P. *Nature* **2000**, *404*, 59.
(5) Hu, J. T.; Odom, T. W.; Lieber, C. M. *Acc. Chem. Res.* **1999**, *32*, 435.
(6) Huynh, W. U.; Dittmer, J. J.; Alivisatos, A. P. *Science* **2002**, *295*, 2425.
(7) Colvin, V. L.; Schlamp, M. C.; Alivisatos, A. P. *Nature* **1994**, *370*, 354.
(8) Coe, S.; Woo, W. K.; Bawendi, M.; Bulovic, V. *Nature* **2002**, *420*, 800.
(9) Beecroft, L. L.; Ober, C. K. *Chem. Mater.* **1997**, *9*, 1302.
(10) Duan, X. F.; Huang, Y.; Agarwal, R.; Lieber, C. M. *Nature* **2003**, *421*, 241.

(11) Bruchez, M.; Moronne, M.; Gin, P.; Weiss, S.; Alivisatos, A. P. *Science* **1998**, *281*, 2013.
(12) Chan, W. C. W.; Nie, S. M. *Science* **1998**, *281*, 2016.
(13) Derfus, A. M.; Chan, W. C. W.; Bhatia, S. N. *Adv. Mater.* **2004**, *16*, 961.
(14) Mokari, T.; Rothenberg, E.; Popov, I.; Costi, R.; Banin, U. *Science* **2004**, *304*, 1787.
(15) Milliron, D. J.; Hughes, S. M.; Cui, Y.; Manna, L.; Li, J. B.; Wang, L. W.; Alivisatos, A. P. *Nature* **2004**, *430*, 190.
(16) Manna, L.; Scher, E. C.; Alivisatos, A. P. *J. Am. Chem. Soc.* **2000**, *122*, 12700.
(17) Peng, Z. A.; Peng, X. G. *J. Am. Chem. Soc.* **2001**, *123*, 183.
(18) Peng, Z. A.; Peng, X. G. *J. Am. Chem. Soc.* **2001**, *123*, 1389.
(19) Peng, Z. A.; Peng, X. G. J. *J. Am. Chem. Soc.* **2002**, *124*, 3343.
(20) Jun, Y.-W.; Lee, S.-M.; Kang, N.-J.; Cheon, J. *J. Am. Chem. Soc.* **2001**, *123*, 5150.
(21) Lee, S.-M.; Cho, S.-N.; Cheon, J. *Adv. Mater.* **2003**, *15*, 441.
(22) Li, Y. D.; Liao, H. W.; Ding, Y.; Fan, Y.; Zhang, Y.; Qian, Y. T. *Inorg. Chem.* **1999**, *38*, 1382.
(23) Yang, J.; Zeng, J.-H.; Yu, S.-H.; Yang, L.; Zhou, G.-E.; Qian, Y.-T. *Chem. Mater.* **2000**, *12*, 3259.
(24) Li, Y. C.; Li, X. H.; Yang, C. H.; Li, Y. F. *J. Mater. Chem.* **2003**, *13*, 2641.
(25) Li, Y.; Huang, F. Z.; Zhang, Q. M.; Gu, Z. N. *J. Mater. Sci.* **2000**, *35*, 5933.
(26) Manna, L.; Milliron, D. J.; Meisel, A.; Scher, E. C.; Alivisatos, A. P. *Nat. Mater.* **2003**, *2*, 382.
(27) Gao, F.; Lu, Q. Y.; Xie, S. H.; Zhao, D. Y. *Adv. Mater.* **2002**, *14*, 1537.
(28) Wang, W. L.; Bai, F. L. *ChemPhysChem* **2003**, *4*, 761.
(29) Zhang, P.; Gao, L. *Langmuir* **2003**, *19*, 208.
(30) Grebinski, J. W.; Hull, K. L.; Zhang, J.; Kosel, T. H.; Kuno, M. *Chem. Mater.* **2004**, *16*, 5260.
(31) Meakin, P. *Fractals, scaling and growth far from equilibrium*; Cambridge University Press: New York, 1998.
(32) Zhang, J.; Sun, L. D.; Yin, J.; Su, H. L.; Liao, C. S.; Yan, C. H. *Chem. Mater.* **2002**, *14*, 4172.

CG050068W